Resolution of Michaelis Complex, Acylation, and Conformational Change Steps in the Reactions of the Serpin, Plasminogen Activator Inhibitor-1, with Tissue Plasminogen Activator and Trypsin[†]

Steven T. Olson,*[,‡] Richard Swanson,[‡] Duane Day,[§] Ingrid Verhamme,[§] Jan Kvassman,[§] and Joseph D. Shore[§]

Center for Molecular Biology of Oral Diseases, University of Illinois at Chicago, Chicago, Illinois 60612, and Henry Ford Hospital, Division of Biochemical Research, Detroit, Michigan 48202

Received April 10, 2001; Revised Manuscript Received July 6, 2001

ABSTRACT: Michaelis complex, acylation, and conformational change steps were resolved in the reactions of the serpin, plasminogen activator inhibitor-1 (PAI-1), with tissue plasminogen activator (tPA) and trypsin by comparing the reactions of active and Ser 195-inactivated enzymes with site-specific fluorescent-labeled PAI-1 derivatives that report these events. Anhydrotrypsin or S195A tPA-induced fluorescence changes in P1′-Cys and P9-Cys PAI-1 variants labeled with the fluorophore, NBD, indicative of a substrate-like interaction of the serpin reactive loop with the proteinase active-site, with the P1′ label but not the P9 label perturbing the interactions by 10−60-fold. Rapid kinetic analyses of the labeled PAI-1-inactive enzyme interactions were consistent with a single-step reversible binding process involving no conformational change. Blocking of PAI-1 reactive loop-β-sheet A interactions through mutation of the P14 Thr → Arg or annealing a reactive center loop peptide into sheet A did not weaken the binding of the inactive enzymes, suggesting that loop-sheet interactions were unlikely to be induced by the binding. Only active trypsin and tPA induced the characteristic fluorescence changes in the labeled PAI-1 variants previously shown to report acylation and reactive loop-sheet A interactions during the PAI-1-proteinase reaction. Rapid kinetic analyses showed saturation of the reaction rate constant and, in the case of the P1′-labeled PAI-1 reaction, biphasic changes in fluorescence indicative of an intermediate resembling the noncovalent complex on the path to the covalent complex. Indistinguishable K_M and k_{lim} values of ∼20 μM and 80−90 s^{-1} for reaction of the two labeled PAI-1s with trypsin suggested that a diffusion-limited association of PAI-1 and trypsin and rate-limiting acylation step, insensitive to the effects of labeling, controlled covalent complex formation. By contrast, differing values of K_M of 1.7 and 0.1 μM and of k_{lim} of 17 and 2.6 s^{-1} for tPA reactions with P1′ and P9-labeled PAI-1s, respectively, suggested that tPA-PAI-1 exosite interactions, sensitive to the effects of labeling, promoted a rapid association of PAI-1 and tPA and reversible formation of an acyl−enzyme complex but impeded a rate-limiting burial of the reactive loop leading to trapping of the acyl−enzyme complex. Together, the results suggest a kinetic pathway for formation of the covalent complex between PAI-1 and proteinases involving the initial formation of a Michaelis-type noncovalent complex without significant conformational change, followed by reversible acylation and irreversible reactive loop conformational change steps that trap the proteinase in a covalent complex.

The serpins are a large superfamily of proteins many of whose members function to regulate the activity of serine or cysteine proteinases in key physiologic processes (*1*, *2*). Such regulation is accomplished by the serpin inhibiting the activity of its target proteinases through the formation of stoichiometric complexes. The mechanism by which serpins form such complexes and inhibit proteinase function is quite novel among protein proteinase inhibitors in that it involves major conformational changes in both the serpin and proteinase (*3*−*6*), formation of a covalent linkage between the interacting proteins (*7*−*9*), and a multistep pathway for complex formation (*10*−*13*). The remarkable differences between the serpin inhibitory mechanism and the simpler lock-and-key type mechanism used by other families of protein proteinase inhibitors (*14*) has been most convincingly demonstrated by a recent structure of a serpin−proteinase complex (*15*). This structure shows the proteinase covalently joined in acyl-linkage to the P1 specificity residue of the serpin reactive center loop through the proteinase active-site serine with cleavage of the P1−P1′ bond in the loop.[1] Moreover, the amino-terminal end of the cleaved loop to which the proteinase is covalently tethered is fully inserted

[†] This work was supported by National Institutes of Health Grants P01 HL-64013 (to S.T.O.) and R01 HL-45930 (to J.D.S.)

* To whom correspondence should be addressed at the Center for Molecular Biology of Oral Diseases, University of Illinois at Chicago, Room 530E Dentistry (M/C 860), 801 S. Paulina Street, Chicago, IL 60612. Tel. (312) 996-1043. Fax (312) 413-1604. E-mail: stolson@uic.edu.

[‡] University of Illinois at Chicago.

[§] Henry Ford Hospital.

10.1021/bi0107290 CCC: $20.00
Published on Web 09/01/2001

as a central strand of β-sheet A of the serpin core, with consequent movement of the proteinase from its initial docking site with the loop to the opposite end of sheet A where it is anchored to the serpin and distorted. While this structure strongly suggests that the serpin inhibitory mechanism involves binding of the proteinase to the serpin reactive loop as a substrate, acylation of the loop, and large conformational changes in both the serpin and proteinase, the kinetic pathway leading to the stable acyl-intermediate complex has remained a point of controversy. Some studies have suggested that a partial or full insertion of the serpin reactive center loop into sheet A can be induced by noncovalent complex formation without the need for acylation and that the rate of this conformational change may limit the rate of covalent complex formation (*12*, *16*, *17*). Reversible and irreversible reactive center loop insertion into sheet A is known to occur in serpins without the need for proteolysis of the loop, most notably in the cases of antithrombin (*18*, *19*) and PAI-1 *(20)*. However, other studies have claimed that proteolysis of the loop is necessary to trigger the serpin reactive loop conformational change and trap the proteinase as a stable acyl−enzyme complex (*4*, *7*, *8*, *15*, *21*−*26*).

Insight into the serpin inhibitory mechanism has come from the use of single cysteine variants of serpins site-specifically labeled with fluorophores to provide reporters of the molecular events that are thought to occur during the serpin−proteinase reaction (*4*, *7*, *13*, *16*, *21*, *25*). It was previously demonstrated that two such derivatives of PAI-1, containing fluorescent labels at the P1′ (*7*) and P9 (*4*) residues of the serpin reactive center loop, underwent fluorescent changes during the reaction with target proteinases which reported acylation and reactive loop conformational change steps. In the present study, we have compared the reactions of these site-specifically labeled PAI-1 derivatives as well as wild-type PAI-1 with both active and Ser 195-inactivated trypsin and tPA using rapid kinetic and equilibrium binding approaches. These studies were undertaken to elucidate the sequence of Michaelis complex, acylation, and reactive loop conformational change steps in PAI-1-proteinase reactions, to resolve those steps involved in noncovalent complex formation from those required for covalent complex formation, and to elucidate the role of tPA-PAI-1 exosite interactions in these events (*27*, *28*). Our findings demonstrate that the inactive enzymes induce fluorescence changes in the labeled PAI-1s indicative of a substrate-like interaction of the serpin reactive loop with the proteinase active-site, with kinetics consistent with a single-step association involving minimal conformational change. Blocking of PAI-1 reactive loop-β-sheet A interactions by mutagenesis or by binding of a reactive loop peptide does not weaken noncovalent PAI-1-inactive enzyme interactions, affirming that reactive loop-sheet A interactions are not involved in stabilizing the noncovalent complex. By contrast, the fluorescence changes reporting acylation and reactive loop-sheet A interactions in the labeled PAI-1-proteinase reactions are only induced by an active enzyme and the kinetics of these changes indicate that they accompany the transformation of an intermediate resembling the noncovalent complex to a covalent complex. Comparison of trypsin and tPA reactions with labeled or wild-type PAI-1 species identifies different rate-limiting steps in the two proteinase reactions and suggests a role for tPA-PAI-1 exosite interactions in enhancing the formation of both noncovalent and covalent complexes.

EXPERIMENTAL PROCEDURES

Expression, Purification, and Fluorescent Labeling of Recombinant PAI-1 Variants. Wild-type and variant recombinant human PAI-1s (P1′ Met → Cys and P9 Ser → Cys) constructed by site-directed mutagenesis were expressed in *Escherichia coli* and purified as described (*4*, *7*). Concentrations of recombinant PAI-1 preparations were determined from the absorbance at 280 nm using an absorption coefficient of 1.0 $(mg/mL)^{-1}$ cm^{-1} and molecular weight of 43 000 (*4*). Labeling of the single Cys PAI-1 variants with iodoacetamide derivatives of the fluorescent probes, NBD or fluorescein (Molecular Probes), was performed as described (*4*, *7*, *13*). Labeling stoichiometries determined from the NBD and protein absorbance (*4*) ranged from 0.8 to 1.3 mol of NBD/mol of PAI-1 in the 4−6 preparations of each labeled PAI-1 used in the present studies. NBD-labeled P1′-Cys PAI-1 was complexed with an octapeptide corresponding to the P14−P7 reactive center loop residues and purified from residual free peptide as described (*24*).

Proteinases. Human tissue plasminogen activator (tPA) and the Ser 195 → Ala variant tPA were recombinant proteins obtained from Genentech that were converted to two-chain forms by treatment with plasmin-linked-agarose as described (*29*) followed by dialysis into 0.5 M Hepes, 0.05 M NaCl, 1 mM EDTA, 0.1% PEG 8000. Concentrations were determined from the 280 nm absorbance using an absorption coefficient of 1.92 $(mg/mL)^{-1}$ cm^{-1} and molecular weight of 66 000 (4). Bovine β-trypsin was purified from commercial tosylphenylalaninechloromethyl ketone-treated trypsin (Sigma Type XIII) by pH gradient elution from SBTI-agarose (*30*). β-Anhydrotrypsin (Ser 195 → dehydroalanine) was prepared by alkaline treatment of phenylmethylsulfonyl-fluoride-modified trypsin (*31*) followed by purification on SBTI-agarose as with the active enzyme (*30*). The anhydro-enzyme was treated with 10 μM FFR-chloromethyl ketone for 15 h in pH 7.4 buffer followed by dialysis into 1 mM HCl to eliminate any residual trypsin. Active and inactive enzymes were stored in 1 mM HCl. Concentrations of trypsin and anhydrotrypsin were initially determined from the 280 nm absorbance using an absorption coefficient of 1.54 $(mg/mL)^{-1}$ cm^{-1} and molecular weight of 23 900 (32). Measurement of the rate of trypsin hydrolysis of a synthetic substrate (S-2222 from Chromogenix) under standard conditions was then used to determine the active-site concentration of the enzyme (>90%) based on the turnover number previously measured for trypsin active-site titrated with fluorescein mono-*p*-guanidinobenzoate (*22*). Titrations of the anhydro-enzyme with SBTI (Sigma) monitored from the fluorescence decrease accompanying the displacement of the bound probe,

[1] Abbreviations: PAI-1, plasminogen activator inhibitor-1; tPA, tissue plasminogen activator; PEG, poly(ethylene glycol); SDS, sodium dodecyl sulfate; PAGE, polyacrylamide gel electrophoresis; P1′, P9, etc., Schechter and Berger nomenclature for reactive loop residues of PAI-1 where P1, P2,... denote residues on the amino-terminal side of the scissile bond and P1′, P2′,... denote residues on the carboxyl side of this bond; SBTI, soybean trypsin inhibitor, NBD, *N*,*N*′-dimethyl-*N*-(acetyl)-*N*′-(7-nitrobenz-3-oxa-1,3-diazol-4-yl) ethylenediamine.

p-aminobenzamidine (Aldrich), from the enzyme active-site (*22*), demonstrated that the inactive enzyme had a full complement of active sites. Activity assay revealed <0.001% residual trypsin in the anhydrotrypsin. Titrations of tPA with wild-type PAI-1 whose functional concentration had been standardized by titration of active-site titrated trypsin (see below) confirmed that tPA was fully functional.

Experimental Conditions. Experiments were performed at 25 °C in pH 7.4 buffers containing either (i) 0.1 M Hepes, 0.1 M NaCl, 0.1% PEG 8000 or (ii) 0.5 M Hepes, 0.05 M NaCl, 1 mM EDTA, 0.1% PEG 8000 as indicated.

Functional PAI-1 Activity. The fraction of labeled or wild-type PAI-1s capable of inhibiting trypsin or tPA through the formation of a stoichiometric complex was determined by titrating fixed levels of enzyme (10−20 nM) with increasing molar ratios of PAI-1 to enzyme up to 1.2−2. Following incubation for 20−60 min, residual enzyme activity was determined by dilution of an aliquot into 100 μM S-2222 (Chromogenix) in the case of trypsin or 100 μM Spectrozyme tPA (American Diagnostica) in the case of tPA followed by the recording of the initial linear rate of absorbance increase at 405 nm. Plots of residual enzyme activity vs the molar ratio of inhibitor to enzyme were linear and provided the functional concentration of inhibitor from the extrapolated *x*-axis intercept of a linear regression fit of the data. Wild-type and labeled PAI-1s did not lose any significant activity over the time frame of experiments conducted in this study.

SDS Gel Electrophoresis. PAI-1s, proteinases, and the complexes they form were analyzed by SDS−PAGE under reducing conditions using a 10% gel and the Laemmli discontinuous buffer system (*33*). Trypsin was inactivated prior to denaturation by treatment with ~300 μM FFR-chloromethyl ketone. Protein bands were visualized by Coomassie Blue R250 staining or by the visible fluorescence emitted from the labeled PAI-1s upon UV excitation using a Fotodyne transilluminator. Quantitation of stained protein bands was done by integration of scanned band intensities using a Nucleovision Imaging Workstation (Nucleotech, Hayward, CA) under conditions where there was a linear relationship between intensity and amount of protein loaded. The PAI-1 contribution to the measured intensity of serpin−proteinase complex bands was calculated by multiplying by the fraction of the total mass of the complex due to PAI-1.

Second-Order Association Rate Constants for PAI-1-Proteinase Reactions. Association rate constants for PAI-1 inhibition of trypsin or tPA were determined under pseudo-first-order conditions using at least a 5-fold molar excess of inhibitor to enzyme by continuously monitoring the decrease in enzyme activity in the presence of a chromogenic or fluorogenic substrate. Conditions were as follows: (i) 0.2−0.7 nM trypsin, 2−20 nM PAI-1, and 200 μM S-2222; (ii) 1−2 nM tPA, 5−20 nM PAI-1, and 400−600 μM Spectrozyme tPA; or (iii) 0.1−0.25 nM tPA, 0.5−3 nM PAI-1, and 50−100 μM methoxy-succinyl-IGR-7-amido-4-methylcoumarin (Enzyme Systems Products). Protein adsorption in these assays was minimized by conducting reactions in polystyrene cuvettes coated with PEG 20000 (*34*). Inhibition progress curves monitored by absorbance at 405 nm or by fluorescence with excitation and emission wavelengths of 380 and 440 nm, respectively, were fitted by a single-exponential function with a finite endpoint to obtain the pseudo-first-order inhibition rate constant, k_{obs} (*23*). The second-order rate constant was calculated by dividing k_{obs} by the functional inhibitor concentration and then multiplying by the factor, $1 + [S]_o/K_M$, to correct for the competitive effect of the substrate on the inhibitor−proteinase reaction. The following measured K_M values were used for this correction: 33 μM for trypsin hydrolysis of S-2222 in 0.1 M Hepes buffer; 91 and 184 μM for tPA hydrolysis of Spectrozyme tPA in 0.1 and 0.5 M Hepes buffers, respectively; and 470 and 1700 μM for tPA hydrolysis of the IGR-coumarin substrate in 0.1 and 0.5 M Hepes buffers, respectively.

Fluorescence Emission Spectroscopy. Emission spectra of 0.05−0.1 μM NBD-labeled PAI-1s in the absence and presence of saturating active and inactive proteinases were recorded in 0.1 and 0.5 M Hepes buffers at 25 °C on an SLM 8000 spectrofluorometer in the ratio mode with excitation at 480 nm, an emission step size of 1−2 nm and band-passes of 4 nm for both excitation and emission beams.

Equilibrium Binding of PAI-1-Proteinase Interactions. Equilibrium binding of inactive and active proteinases to NBD-labeled PAI-1 derivatives was measured by titrating a fixed level of the fluorescent-labeled PAI-1 (0.05−0.1 μM) with proteinases and monitoring the fluorescence change at excitation and emission wavelengths of 480 nm (4 nm band-pass) and 530 nm (16 nm band-pass). Fluorescence readings were corrected for a buffer blank and dilution and expressed as $\Delta F_{obs}/F_o = (F_{obs} - F_o)/F_o$ where F_{obs} and F_o are observed and initial fluorescence readings, respectively. The fluorescence changes induced by active enzyme binding were stoichiometric and fit by linear regression. The saturable changes in fluorescence induced by inactive proteinases were fit by the quadratic equilibrium binding equation to obtain values for the dissociation constant, K_D, the maximal relative fluorescence change, $\Delta F_{max}/F_o$ and, in the case of the P9-NBD-PAI-1 interaction with S195A tPA in 0.1 M Hepes buffer, a stoichiometric factor for the PAI-1 concentration (*35*). Binding of wild-type PAI-1 to S195A tPA was analyzed by competitive binding titrations in which P1′-NBD-PAI-1 was first titrated with the inactive enzyme with binding monitored by the NBD fluorescence increase, followed by titrating with wild-type PAI-1 and monitoring the fluorescence decrease as the labeled PAI-1 is displaced from the inactive enzyme complex by the unlabeled PAI-1. Relative fluorescence changes in this case were fit by the cubic competitive binding equation (*35*) with K_D, a stoichiometric factor for the wild-type PAI-1 interaction and $\Delta F_{max}/F_o$ as the fitted parameters and with K_D and the stoichiometry for the labeled PAI-1 interaction fixed at the values determined in direct titrations. Kinetically determined values of K_D for PAI-1 interactions with anhydrotrypsin and S195A tPA were determined by analyzing the effect of the inactive enzyme on k_{obs} for PAI-1 inhibition of the active enzyme under pseudo-first-order conditions. The wild-type PAI-1−anhydrotrypsin interaction was quantitated in 0.1 M Hepes buffer from the effects of 50−800 nM anhydrotrypsin on the rate of inactivation of 0.5 nM trypsin by 4 nM PAI-1. Trypsin inactivation was measured by discontinuously assaying aliquots of reaction mixtures for residual enzyme activity from the initial rate of hydrolysis of 50 μM Tosyl-GPR-7-amido-4-methylcoumarin. The loss in enzyme activity was

fit by a single-exponential decay to obtain k_{obs} and the decrease in k_{obs} produced by anhydrotrypsin was fit by the equation: $k_{obs}/k_{obs,o} = K_D/(K_D + [E^*]_o)$ where $k_{obs,o}$ represents k_{obs} determined in the absence of anhydrotrypsin, K_D is the dissociation constant for the PAI-1−anhydrotrypsin interaction and $[E^*]_o$ is the anhydrotrypsin concentration. The wild-type PAI-1−tPA interaction was quantitated in 0.1 M Hepes buffer from the effects of 5−20 nM S195A tPA on the rate of inactivation of 2 nM tPA by 10 nM PAI-1. tPA inactivation was measured in the presence of 500 μM Spectrozyme tPA from the exponential decrease in the rate of substrate hydrolysis as described above for measuring the second-order inhibition rate constant. The dependence of k_{obs} on S195A tPA concentration was then fit by the equation,

$$k_{obs}/k_{obs,o} = ([E^*]_{eff} - [I]_o + K_D - (([E^*]_{eff} + [I]_o + K_D)^2 - 4[E^*]_{eff}[I]_o)^{1/2})/(2[I]_o)$$

where $[I]_o$ is the PAI-1 concentration, $[E^*]_{eff}$ is the effective S195A tPA concentration corrected for the fraction bound to the chromogenic substrate, and K_D is the dissociation constant for the PAI-1−S195A tPA interaction. $[E^*]_{eff}$ was estimated by dividing $[E^*]_o$ by a correction factor of $1 + [S]_o/K_M$.

Stopped-Flow Kinetics of PAI-1-Proteinase Interactions. The kinetics of binding active and inactive enzymes to wild-type and fluorescent-labeled variant PAI-1 species were studied under pseudo-first-order conditions by stopped-flow fluorometry in an Applied Photophysics SX-17MV instrument as in previous studies (*4*, *7*). NBD-labeled PAI-1 (5−100 nM for P9-NBD-PAI-1 and 20−100 nM for P1′-NBD-PAI-1) was reacted with a 5-fold or higher molar excess of proteinase, and the fluorescence change accompanying the reaction was monitored with excitation at 480 nm (8 nm band-pass) and a cutoff emission filter which passed light above 520 nm. For trypsin reactions, PAI-1 samples were made up in a 2-fold concentrated buffer and the enzyme was in 1 mM HCl. For tPA reactions, both PAI-1 and the enzyme were made up in the same reaction buffer. Wild-type PAI-1 inhibition of proteinases was studied by monitoring the fluorescence decrease due to displacement of the probe, *p*-aminobenzamidine, from the enzyme active site by the inhibitor as in previous studies (*10*), by including 10 or 200 μM *p*-aminobenzamidine with the enzyme in the case of trypsin and tPA reactions, respectively. For these reactions, the inhibitor concentration was varied with at least a 5-fold molar excess of inhibitor over enzyme. The competitive effect of *p*-aminobenzamidine on the enzyme−inhibitor reaction was corrected for by expressing inhibitor concentrations as effective concentrations obtained by dividing by the factor, $1 + [p\text{-aminobenzamidine}]_o/K_D$, where K_D is the dissociation constant for *p*-aminobenzamidine binding to the enzyme. A previously measured K_D of 8.5 μM for the trypsin interaction (*22*) and an average K_D of 200 ± 40 μM measured for the tPA interaction by direct binding or by competitive inhibition of chromogenic substrate hydrolysis (*22*), were used for these calculations. Fluorescence changes were monitored in this case by exciting at 325 nm and using a cutoff emission filter which transmitted light above 350 nm.

Fluorescence changes accompanying labeled and unlabeled PAI-1-proteinase reactions in most cases were satisfactorily fit by a single-exponential function except as noted below. A total of 5−15 reaction traces were collected for each set of concentrations and the exponential fits were averaged to obtain the observed pseudo-first-order rate constant, k_{obs}. Reactions of P9-NBD-PAI-1 with trypsin and tPA exhibited brief lags of < 50 ms at high enzyme concentrations (≥ 5 μM trypsin and ≥ 0.1 μM tPA) which could not be reliably quantitated as a separate reaction phase. The subsequent observable fluorescence change was well fit by a single-exponential process, except for tPA reactions with P9-NBD-PAI-1 in the high tPA concentration range which showed a slow linear increase of fluorescence amounting to <10% of the total fluorescence change, as previously noted (*4*). The exponential fluorescence change was fit in the latter case by assuming a finite linear fluorescence change as the endpoint. The minor fluorescence changes at the end of these reactions were considered to represent a process after the primary fluorescence change reporting reactive loop insertion into sheet A, possibly involving a slow isomerization of the fluorophore, based on the finding that the rate of SDS-stable complex formation measured by rapid quenching coincides with the rate of the primary P9 fluorescence change (*4*, *24*). The dependence of k_{obs} for the predominant exponential phase in these reactions on enzyme concentration was fit by the equation for the two-step binding mechanism,

$$E + I \underset{k_{off}}{\overset{k_{on}}{\rightleftharpoons}} E{-}I \xrightarrow{k_{lim}} E{-}I^*$$

where E designates the enzyme and I the inhibitor, k_{on} and k_{off} are forward and reverse rate constants for formation and dissociation of the intermediate complex, and k_{lim} is the rate constant for conversion of the intermediate complex to the final complex. When the observable fluorescence change is associated with the second step, k_{obs} will increase with enzyme concentration in accordance with the equation (*13*)

$$k_{obs} = k_{lim}[E]_o/(K_M + [E]_o)$$

where K_M is the concentration of enzyme at which k_{obs} reaches half of k_{lim} and is given by $(k_{lim} + k_{off})/k_{on}$. Fitting of data to this equation yielded values for K_M and k_{lim}.

The reaction of P1′-NBD-PAI-1 with tPA was distinctly biphasic with a rapid fluorescence increase followed by a slower fluorescence decrease. In this case, the time dependence of the changes in the observed fluorescence (F_{obs}) was fit by the two exponential function,

$$F_{obs} = F_\infty + \Delta F_1 \exp(-k_{obs,1}t) + \Delta F_2 \exp(-k_{obs,2}t)$$

where F_∞, ΔF_1, and ΔF_2 are the endpoint fluorescence, the fluorescence change for the fast phase and fluorescence change for the slow phase, respectively, and $k_{obs,1}$ and $k_{obs,2}$ are the observed pseudo-first-order rate constants for the fast and slow phases, respectively. The dependence of rate constants and fluorescence amplitude changes on enzyme concentration were analyzed by computer fitting to the equations below governing the above two-step reaction model for formation of the enzyme−inhibitor complex (*36*).

$$k_{obs,1} = (k_{on}[E]_o + k_{off} + k_{lim} + ((k_{on}[E]_o + k_{off} + k_{lim})^2 - 4k_{on}[E]_o k_{lim})^{1/2})/2$$

$$k_{obs,2} = (k_{on}[E]_o + k_{off} + k_{lim} - ((k_{on}[E]_o + k_{off} + k_{lim})^2 - 4k_{on}[E]_o k_{lim})^{1/2})/2$$

$$\Delta F_1/[PAI\text{-}1]_o = (-k_{on}[E]_o/(k_{on}[E]_o + k_{off} + k_{lim})) \times ((k_{lim}(\Phi_{EI*} - \Phi_I)/(k_{on}[E]_o + k_{off} + k_{lim})) - (\Phi_{EI} - \Phi_I))$$

$$\Delta F_2/[PAI\text{-}1]_o = (k_{on}[E]_o/(k_{on}[E]_o + k_{off} + k_{lim})) \times (\Phi_{EI} - \Phi_I) - (\Phi_{EI*} - \Phi_I)$$

where Φ_I, Φ_{EI}, and Φ_{EI*} are the fluorescence coefficients representing the fluorescence per unit concentration of free P1′-NBD-PAI-1, its noncovalent complex with tPA and its covalent complex with the enzyme, respectively. The latter two equations were used to fit the fluorescence coefficient of the intermediate noncovalent complex species by fixing values for the coefficients of the free inhibitor and the final covalent complex using measured values of the starting and endpoint fluorescence normalized to the PAI-1 concentration. When $k_{obs,1} \gg k_{obs,2}$, the above equations for $k_{obs,1}$ and $k_{obs,2}$ reduce to the linear and hyperbolic forms,

$$k_{obs,1} = k_{on}[E]_o + k_{off} + k_{lim}$$

$$k_{obs,2} = k_{lim}[E]_o/(K_M + [E]_o)$$

Kinetic data were also fit with these equations.

Simulations of the PAI-1-tPA reaction according to the model of Scheme 2 were done by numerical integration of the differential equations for this model using the program Scientist (Micromath).

RESULTS

Characterization of NBD-Labeled PAI-1 Species. SDS gel electrophoretic analysis of the reactions of wild-type PAI-1 and labeled PAI-1 variants with a molar excess of tPA (Figure 1) showed that the labeled PAI-1 derivatives were functional in forming SDS-stable complexes. However, more reactive center loop cleaved PAI-1 was produced in the reaction of tPA with the P9-labeled PAI-1 than with the wild-type or P1′-labeled-PAI-1. Quantitation of the relative amounts of PAI-1 in complex versus cleaved bands or titrations of the amount of PAI-1 required to completely inhibit proteinase activity confirmed that P9-NBD-PAI-1 inhibited two-chain tPA as well as β-trypsin with stoichiometries somewhat elevated relative to wild-type or P1′-NBD-PAI-1 reactions with these enzymes (Table 1). Small amounts of latent unreactive PAI-1 were also evident in the preparations following reaction with tPA (Figure 1). On the basis of these findings, functional concentrations of PAI-1 representing the fraction of total serpin reacting through the inhibitory pathway were determined from measured stoichiometries of inhibition (*1*) (see Experimental Procedures). Using these functional inhibitor concentrations, second-order association rate constants for inhibition of trypsin and tPA by the labeled PAI-1 species were found to be similar to or only modestly reduced from the values for wild-type PAI-1 inhibition of these enzymes, in keeping with previous findings (*4*, *7*) (Table 1).

Visualization of protein bands in the SDS gel in Figure 1 by fluorescence confirmed the presence of the fluorophore in each labeled PAI-1 and showed the fate of the label upon forming complexes with tPA. In the case of P9-NBD-PAI-1, the label appeared in the tPA complexed and cleaved serpin bands, whereas with P1′-NBD-PAI-1 the label was not present in either the complexed or cleaved serpin bands but instead appeared in a low molecular weight peptide band. This was most evident when a fluorescein derivative of P1′-Cys-PAI-1 was reacted with excess tPA (Figure 1). Only the unreacted latent PAI-1 and peptide bands were fluorescent, consistent with cleavage of the P1−P1′ bond and release of the P1′-NBD label with the ~5 kDa C-terminal peptide product of cleavage in both the PAI-1−tPA complex and cleaved PAI-1 bands (*7*−*9*).

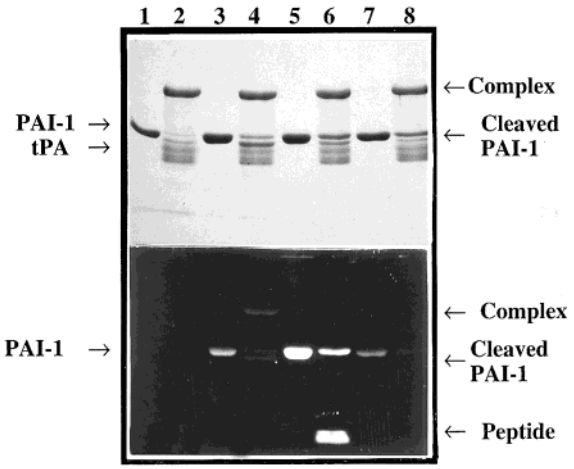

FIGURE 1: SDS−PAGE analysis of fluorescent-labeled PAI-1s and their complexes with tPA. PAI-1s (3 μg) were incubated in the absence (lanes 1, 3, 5, and 7) and presence (lanes 2, 4, 6, and 8) of a 1.2-fold molar excess of tPA for 2 min prior to electrophoresis: wild-type PAI-1 (lanes 1 and 2), P9-Cys-NBD-PAI-1 (lanes 3 and 4), P1′-Cys-fluorescein-PAI-1 (lanes 5 and 6), and P1′-Cys-NBD-PAI-1 (lanes 7 and 8). In the upper gel, protein bands were visualized by Coomassie staining and in the lower gel, bands were visualized by fluorescence. The multiple bands seen with free tPA reflect the glycosylation heterogeneity of the recombinant protein.

Fluorescence Changes Accompanying Binding of Active and S195-Inactivated Proteinases to Labeled PAI-1 Derivatives. Addition of inactive Ser 195 → dehydroAla trypsin or Ser 195 → Ala tPA to P1′-NBD PAI-1 enhanced the fluorescence emission spectrum of the reporter fluorophore maximally to similar extents of 1.9- and 2.3-fold, respectively, and blue-shifted the spectrum by 3−10 nm (Figure 2). By contrast, active trypsin and tPA both quenched the P1′-NBD-PAI-1 fluorescence emission spectrum by ~20% at saturating levels with little change in the emission maximum (Figure 2). These results indicated marked differences in the mode of interaction of inactive versus active forms of tPA and trypsin with the labeled serpin, with the two active or inactive proteinases behaving similarly.

Similar findings were made for the interactions of inactive and active enzymes with P9-NBD-PAI-1. Thus, addition of saturating levels of Ser 195-modified trypsin or tPA to P9-NBD-PAI-1 produced similar small enhancements of 1.2- to 1.4-fold and minimal shifts in the NBD fluorescence emission spectrum whereas active trypsin and tPA maximally induced large 6−7-fold enhancements and 15−20 nm blue-shifts in the emission spectrum (Figure 2).[2] The latter changes were previously shown to report the serpin reactive center loop conformational change which is responsible for the trapping of proteinases in covalent complexes (*4*). The failure

Table 1: Kinetic Parameters and Stoichiometries for the Reactions of Wild-Type, P1′-Cys-NBD, and P9-Cys-NBD PAI-1s with Trypsin or tPA at pH 7.4, 25 °C

PAI-1	enzyme	[Hepes] (M)	K_M[a] (μM)	k_{lim}[a] (s^{-1})	k_{lim}/K_M[a] ($\mu M^{-1}.s^{-1}$)	k_{assoc}[b] ($\mu M^{-1}.s^{-1}$)	SI[c] (mol I/mol E)
wild-type	trypsin	0.1				2.1 ± 0.1	1.2 ± 0.1
P1′-NBD	trypsin	0.1	18 ± 2	88 ± 6	4.9 ± 0.8	2.7 ± 0.1	1.2 ± 0.1
P9-NBD	trypsin	0.1	19 ± 3	81 ± 9	4.3 ± 1.2	3.2 ± 0.2	1.5
wild-type	tPA	0.1				23 ± 1	1.3 ± 0.1
P1′-NBD	tPA	0.1	1.7 ± 0.3	17 ± 2	10 ± 3	7.1 ± 0.5	1.2 ± 0.1
P9-NBD	tPA	0.1	0.10 ± 0.01	2.6 ± 0.1	26 ± 4	14 ± 1	1.8 ± 0.1
wild-type	tPA	0.5				5.2 ± 0.2	
P1′-NBD	tPA	0.5	12 ± 2	16 ± 2	1.3 ± 0.4	1.5 ± 0.1	
P9-NBD	tPA	0.5	0.79 ± 0.01	4.9 ± 0.1	6.2 ± 0.2	3.9 ± 0.1	

[a] Measured from the rapid kinetic experiments of Figure 6 in 0.1 M Hepes buffer and from similar experiments in 0.5 M Hepes buffer. [b] Calculated by dividing k_{obs} for inhibition of enzyme activity by the functional PAI-1 concentration as described in Experimental Procedures. [c] Stoichiometry of inhibition measured by titration of fixed levels of enzyme with PAI-1 as described in Experimental Procedures. Average values ± SE from at least three titrations are reported except for the P9-NBD-PAI-1 reaction with trypsin in which case a single titration was done. Similar results were obtained by integrating the relative amounts of PAI-1 in complex versus cleaved bands on SDS gels (not shown).

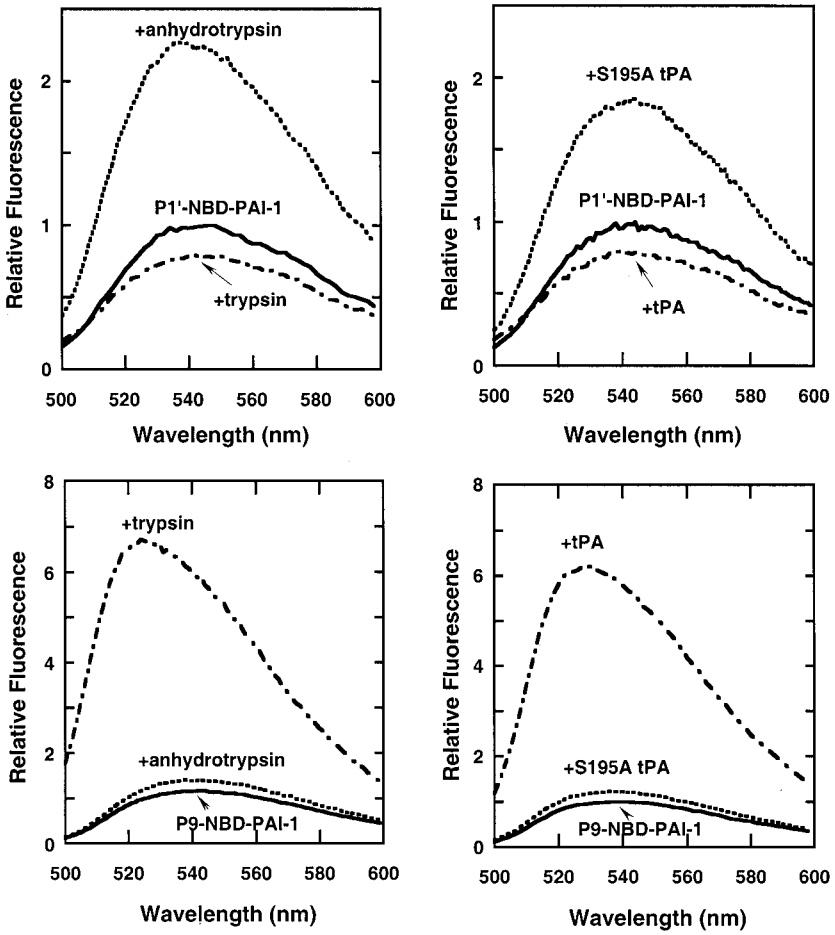

FIGURE 2: Fluorescence emission spectra of fluorescent-labeled PAI-1s and their complexes with Ser 195-inactivated and active proteinases. Emission spectra of 0.1 μM P1′-NBD-PAI-1 (top panels) and of 0.05−0.1 μM P9-NBD-PAI-1 (bottom panels) taken before and after addition of ~20−60 molar equivalents of anhydrotrypsin or ~2 equiv of trypsin (left panels), or of ~2−10 equiv of S195A tPA or ~2 equiv of tPA (right panels), as described in Experimental Procedures.

of both inactive enzymes to induce these large fluorescence changes indicated that the proteinase catalytic serine is necessary for triggering this serpin conformational change, in agreement with previous findings (*22*). SDS gel electrophoresis showed that the inactive enzymes were unable to form covalent complexes with labeled or wild-type PAI-1s in contrast to the active enzymes, consistent with the serpin complexes with the inactive enzymes being noncovalent.

Binding of Inactive and Active Enzymes to Fluorescent-Labeled PAI-1 Derivatives. Titrations of the spectral changes induced in the labeled PAI-1 species by active proteinases indicated a tight, stoichiometric binding to the labeled serpins, consistent with the measured stoichiometries of serpin

[2] Lesser fluorescence enhancements were induced in some P9-NBD-PAI-1 preparations by the active enzymes due to variable small amounts of latent inhibitor produced during the labeling procedure which enhanced the basal fluorescence. All preparations behaved indistinguishably with regard to their interactions with the active enzymes.

inhibition and the effective irreversibility of active enzyme binding. By contrast, titrations of the spectral changes induced in the labeled PAI-1 derivatives by the Ser 195-modified enzymes revealed a progressive approach to a maximum fluorescence change requiring in most cases more than one molar equivalent of inactive enzyme to achieve this maximum. The latter behavior indicated a reversible equilibrium binding of the inactive enzymes to the labeled PAI-1s. Binding curves for the interactions of P1′-NBD-PAI-1 with anhydrotrypsin and S195A tPA indicated K_D values of 2.9 ± 0.1 μM and 73 ± 5 nM, respectively, for the interactions (Figure 3). The large fluorescence enhancements accompanying these interactions allowed us to determine the affinity of unlabeled wild-type PAI-1 for the inactive enzymes by competitve binding experiments. Figure 3 shows that the enhanced fluorescence of P1′-NBD-PAI-1 complexed with S195A tPA at two different levels of complex saturation was fully reversed upon titration with wild-type PAI-1, consistent with the unlabeled serpin displacing S195A tPA from its complex with the labeled serpin. Fitting of these curves by the equation for competitive binding yielded indistinguishable K_D values of 0.9 ± 0.1 nM and 1.1 ± 0.1 nM and stoichiometries of 1.1−1.2 mol of S195A tPA/mol of PAI-1 for the wild-type PAI-1−S195A tPA interaction. The P1′-NBD label thus reduced the affinity of PAI-1 for S195A tPA by ~60-fold. Direct measurements of the binding of anhydrotrypsin to wild-type PAI-1 monitored by displacement of the fluorescent probe, *p*-aminobenzamidine, from the enzyme active site, similarly revealed that the P1′ label reduced the affinity of PAI-1 for anhydrotrypsin by 13-fold (Table 2). Titrations of the smaller fluorescence enhancement of P9-NBD-PAI-1 induced by the binding of S195A tPA revealed a high-affinity binding interaction with K_D of ~0.4 nM, similar to that found for the wild-type PAI-1 interaction.

Table 2 summarizes the K_D values obtained for the binding of S195A tPA and anhydrotrypsin to P1′NBD-, P9-NBD-, and wild-type PAI-1s. S195A tPA interactions were measured in both 0.1 and 0.5 M Hepes buffers because of the much greater solubility of tPA in the 0.5 M Hepes buffer (*37*) and desire to confirm the relative affinities of tPA and S195A tPA for wild-type and labeled PAI-1 measured in 0.1 M Hepes. Although binding interactions were weakened in the 0.5 M Hepes buffer, S195A tPA bound wild-type PAI-1 and P9-NBD-PAI-1 with similar affinities, whereas it bound P1′-NBD-PAI-1 ~50-fold more weakly. Corroborating these findings, anhydrotrypsin and S195A tPA were found to decrease the observed pseudo-first-order rate constant for PAI-1 inhibition of trypsin or tPA, respectively, in a manner consistent with competitive binding of the inactive enzyme to PAI-1 with a K_D of 0.41 ± 0.03 μM for the anhydrotrypsin interaction and an estimated K_D of 0.6 ± 0.2 nM for the S195A tPA interaction, reasonably close to the measured K_D values (Table 2). Together, these data showed that the P1′ label markedly affected the affinity of PAI-1 for the inactive enzymes, whereas the P9 label had minimal effects on these interactions.

Binding of S195-Modified Enzymes to Native and Conformational Change-Blocked Forms of PAI-1. Binding of S195A proteinases to the reactive center loop of serpins has been proposed to induce limited or full insertion of the loop into β-sheet A of the serpin and a consequent locking of the loop in a canonical conformation more optimal for proteinase

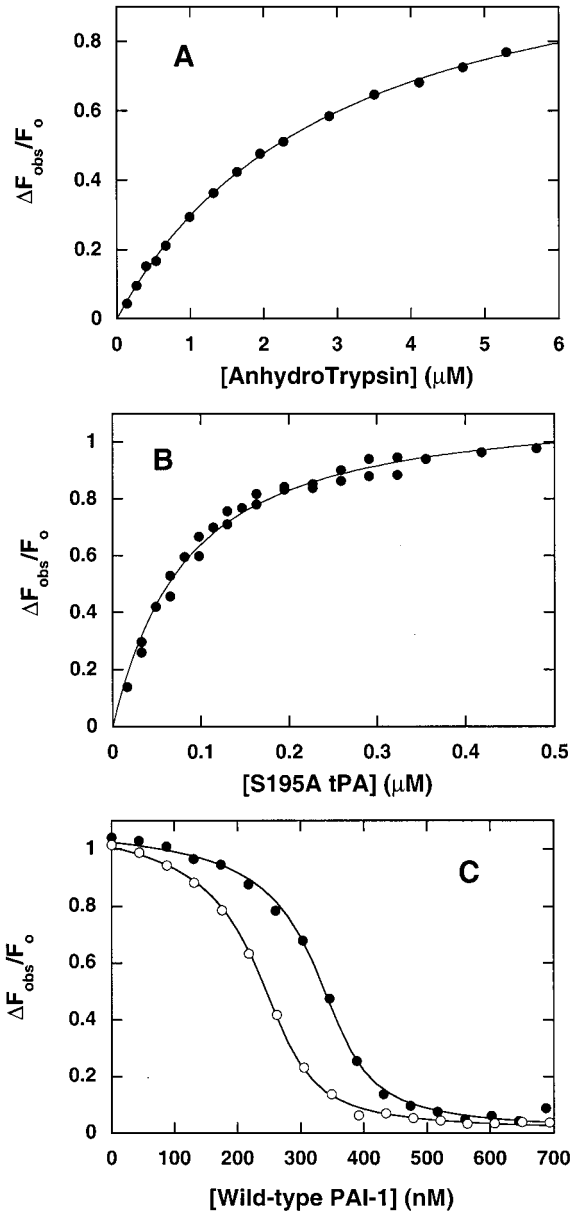

FIGURE 3: Titrations of P1′-NBD-PAI-1 and wild-type PAI-1 interactions with Ser 195-inactivated proteinases. Shown are the fluorescence changes accompanying the titrations of (i) 0.1 μM P1′-NBD-PAI-1 with anhydrotrypsin (panel A), (ii) 0.1 μM P1′-NBD-PAI-1 with S195A tPA (panel B), or (iii) P1′-NBD-PAI-1-S195A tPA complex, formed with 0.05 μM serpin and either 0.32 μM enzyme (open circles) or 0.48 μM enzyme (closed circles), with wild-type PAI-1 (panel C). Titrations were performed as described in Experimental Procedures. Solid lines are nonlinear regression fits of data to the quadratic equilibrium binding equation (panels A and B) or to the cubic competitive binding equation (panel C) given in ref *35*.

interaction (*12*, *17*). To determine whether the binding of Ser 195-modified enzymes to PAI-1 induced the serpin reactive center loop to insert into sheet A, we compared the binding of the catalytically inactive enzymes to native and to conformational change-blocked forms of PAI-1 which could not undergo loop insertion (*24*, *38*). If the binding of the S195A enzyme to PAI-1 induced reactive center loop insertion which stabilized the interaction, then we expected that the affinity of the complex would be decreased by blocking the insertion. Loop insertion-disabled forms of PAI-1 were obtained as in previous studies either by

Table 2: Association and Dissociation Rate Constants and Dissociation Equilibrium Constants for Wild-Type, P1′-Cys-NBD, and P9-Cys-NBD PAI-1 Interactions with Anhydrotrypsin and S195A tPA at pH 7.4, 25 °C[a]

PAI-1	enzyme	[Hepes] M	k_{on} (μM^{-1} s^{-1})	k_{off} (s^{-1})	k_{off}/k_{on} (μM)	K_D[b] (μM)
wild-type	Anhydrotrypsin	0.1				0.23 ± 0.02[c]
P1′-NBD	Anhydrotrypsin	0.1	1.5 ± 0.1	3.5 ± 0.1	2.4 ± 0.2	2.9 ± 0.1
P9-NBD	Anhydrotrypsin	0.1	1.1 ± 0.1	0.40 ± 0.03	0.36 ± 0.06	
wild-type	S195A tPA	0.1				0.0013 ± 0.0004
P1′-NBD	S195A tPA	0.1	14 ± 1	1.1 ± 0.2	0.079 ± 0.020	0.073 ± 0.005
P9-NBD	S195A tPA	0.1	27 ± 1	<1	<0.060	0.0004 ± 0.0001
wild-type	S195A tPA	0.5				0.008 ± 0.001
P1′-NBD	S195A tPA	0.5	1.6 ± 0.1	0.81 ± 0.02	0.51 ± 0.04	0.33 ± 0.01
P9-NBD	S195A tPA	0.5	4.5 ± 0.1	<0.1	<0.02	0.006 ± 0.003

[a] k_{on} and k_{off} values were determined either from the rapid kinetic experiments in Figure 5 in 0.1 M Hepes buffer or from similar experiments in 0.5 M Hepes buffer. K_D values for labeled and unlabeled PAI-1-inactive enzyme interactions were determined from direct or competitive binding titrations such as those shown in Figure 3. Further details are given in Experimental Procedures. [b] Fitted value ± SE from the global fitting of two titrations except for the anhydrotrypsin interaction with P1′-NBD-PAI-1 which represents a single titration. [c] Taken from ref *22*.

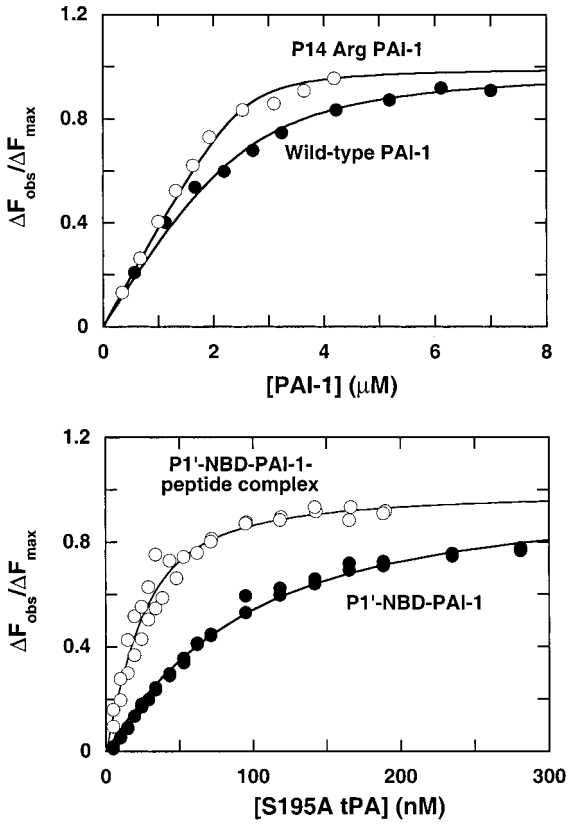

FIGURE 4: Binding of Ser 195-inactivated proteinases to wild-type and conformational change-blocked forms of PAI-1. Shown are the fluorescence changes accompanying the titrations of a mixture of 2.5 μM anhydrotrypsin and 100 μM *p*-aminobenzamidine with wild-type (solid circles) or with P14 Thr → Arg PAI-1 (open circles), as taken from a previous study (*22*) (top panel). The bottom panel shows titrations of 0.1 μM P1′-NBD-PAI-1 either uncomplexed (solid circles) or complexed with a reactive loop octapeptide (open circles) with S195A tPA. Solid lines are fits of data either by a competitive binding equation described previously (*22*) (top panel) or by the quadratic binding equation (*35*) (bottom panel).

annealing a reactive center loop peptide into sheet A (*24*) or by mutating the P14 hinge residue from Thr to Arg (*13*, *38*). Biochemical studies confirm the similar behavior of such modified PAI-1s as proteinase substrates due to the defect in loop-sheet interactions (*13*, *24*, *38*), and the crystal structures of serpin−peptide complexes clearly show the reactive loop to be fully exposed with the peptide blocking the sheet A interaction site (*44*). Figure 4 compares the binding of S195A tPA to native P1′-NBD-PAI-1 and a complex of the labeled PAI-1 with a reactive center loop octapeptide followed from the fluorescence enhancement accompanying the interaction of the inactive enzyme with the fluorescent-labeled PAI-1. Also shown is the binding of anhydrotrypsin to wild-type and P14 Arg PAI-1 measured by displacement of the active-site probe, *p*-aminobenzamidine, from the enzyme active-site, as determined in a previous study (*22*, *38*). Anhydrotrypsin and S195A tPA bound the modified PAI-1s with K_D values of 41 ± 16 nM and 13 ± 5 nM, representing binding affinities ~5-fold higher than those measured for the native serpin. These findings reveal that blocking PAI-1 reactive loop insertion into sheet A does not destabilize PAI-1-inactive enzyme interactions, implying that loop insertion is not likely to be involved in stabilizing these complexes.

Kinetics of PAI-1−Proteinase Interactions. Figure 5 shows an analysis of the kinetics of binding of inactive S195A tPA and anhydrotrypsin to P1′- and P9-labeled PAI-1s in 0.1 M Hepes buffer under pseudo-first-order conditions in which the enzyme was in large molar excess over the labeled serpin. The rate of the fluorescence change was in all cases described well by a single-exponential process. The observed pseudo-first-order rate constant (k_{obs}) increased linearly with increasing enzyme concentration over the concentration range examined, indicating a simple one-step reversible bimolecular interaction. Similar findings were made when the kinetics of S195A tPA binding to the labeled PAI-1s was studied in 0.5 M Hepes buffer. Table 2 summarizes the k_{on} and k_{off} values measured from the slopes and intercepts of the linear plots of k_{obs} vs enzyme concentration. The ratio of k_{off}/k_{on} agreed reasonably well within experimental error with the K_D values measured from equilibrium binding titrations. Moreover, the weaker affinities of S195A tPA for the labeled PAI-1s in 0.5 M Hepes buffer relative to 0.1 M Hepes buffer (Table 2) was principally due to a decrease in k_{on}.

The kinetics of binding of active proteinases to P1′- and P9-labeled PAI-1s was also measured in 0.1 M Hepes buffer under pseudo-first-order conditions in which the enzyme was in large molar excess over the inhibitor. The fluorescence changes essentially conformed to a single-exponential process for the reactions of trypsin and tPA with P9-NBD-PAI-1 and for the reaction of trypsin with P1′-NBD-PAI-1, although brief lags of less than 50 ms were evident in P9-NBD-PAI-1 reactions at higher enzyme concentrations suggestive of the accumulation of an intermediate. Evidence for an intermediate was clearly seen in the reaction of tPA with P1′-NBD-

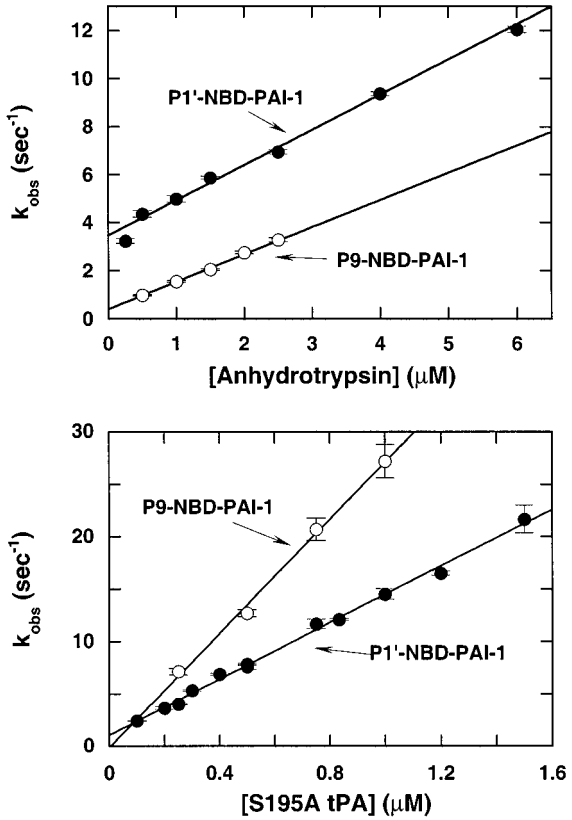

FIGURE 5: Kinetics of binding of Ser 195-inactivated proteinases to fluorescent-labeled PAI-1s. The observed pseudo-first-order rate constant (k_{obs}) ± SE for the binding of anhydrotrypsin (top panel) or S195A tPA (bottom panel) to 0.02−0.1 μM P1′-NBD-PAI-1 (solid circles) or to 0.05−0.1 μM P9-NBD-PAI-1 (open circles) is plotted as a function of the proteinase concentration. k_{obs} was measured from the exponential change in fluorescence after mixing the fluorescent-labeled PAI-1s with the indicated concentrations of proteinase. Solid lines are linear regression fits of the data.

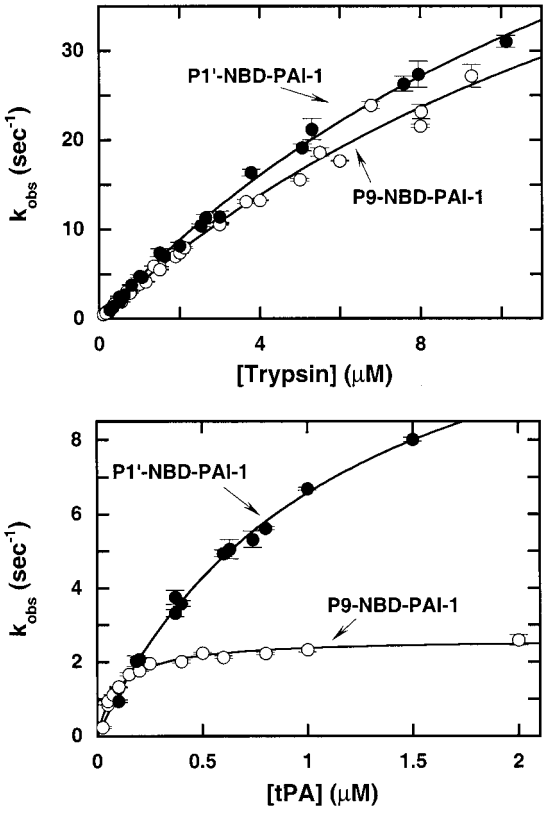

FIGURE 6: Kinetics of binding of active proteinases to fluorescent-labeled PAI-1s. k_{obs} ± SE for the binding of trypsin (top panel) or tPA (bottom panel) to 0.05−0.1 μM P1′-NBD-PAI-1 (solid circles) or to 0.005−0.04 μM P9-NBD-PAI-1 (open circles) is plotted as a function of the proteinase concentration. k_{obs} was measured from the observable exponential fluorescence change in both trypsin reactions and in the tPA reaction with P9-labeled PAI-1 and from the slow exponential fluorescence change in the case of the tPA reaction with P1′-labeled PAI-1 as described in Experimental Procedures. Solid lines are fits to the hyperbolic equation for a two-step binding mechanism.

PAI-1 from the observation of a very rapid exponential increase in fluorescence followed by a slower exponential decay of fluorescence (Figure 7). Contrasting the linear dependence of k_{obs} on enzyme concentration found for the inactive enzyme reactions with the labeled PAI-1s, k_{obs} for the monophasic reactions of the active enzymes with the labeled PAI-1s and for the slow phase of the biphasic reaction was found to increase in a saturable manner as the enzyme concentration was increased (Figure 6). Similar findings were made when tPA reactions with the labeled PAI-1s were conducted in 0.5 M Hepes buffer, indicating that limiting tPA solubility was not responsible for the observed saturation. These observations indicated that the active enzyme reactions were all two-step processes in which an intermediate complex was reversibly formed prior to conversion to an inhibited covalent serpin−enzyme complex with the observable fluorescence changes reporting the latter conversion. Fitting of the data by the expected hyperbolic saturation function provided K_M values reflecting the steady-state formation of the intermediate complex and k_{lim} values indicating the first-order rate constant for the transformation of the intermediate complex to the covalent complex (Table 1). Indistinguishable values of K_M and k_{lim} were found for the reactions of trypsin with P1′- and P9-labeled PAI-1, whereas the values of these kinetic parameters for the reactions of tPA with the two labeled PAI-1 species were very different when measured in either 0.1 or 0.5 M Hepes buffers (Table 1). Reasonable agreement was found between second-order rate constants calculated from the ratio of k_{lim}/K_M and those measured directly, given the errors in determining the former parameters (Table 1). Although K_M values were higher in 0.5 M Hepes than in 0.1 M Hepes for PAI-1-tPA reactions, similar k_{lim} values were found in the two buffers.

The biphasic fluorescence changes observed for the reaction of tPA with P1′-NBD-PAI-1 provided direct evidence that the active enzyme reaction with the fluorescent-labeled PAI-1 is a two-step process. Comparison of fluorescence progress curves for the reactions of S195A tPA and active tPA with P1′-NBD-PAI-1 revealed an initial rapid exponential increase in fluorescence for the tPA reaction which was of lower amplitude than the monoexponential increase in fluorescence seen for the S195A tPA reaction and which was completed much faster (~50 ms for the tPA reaction vs ~500 ms for the S195A tPA reaction) (Figure 7). This was followed by a slower exponential quenching of fluorescence, analogous to that observable for the monoexponential reaction of trypsin with P1′-NBD-PAI-1, which was complete within ~1 s. The final fluorescence changes were in accord with those observed to occur in the emission spectra of Figure 2. Such biphasic fluorescence changes

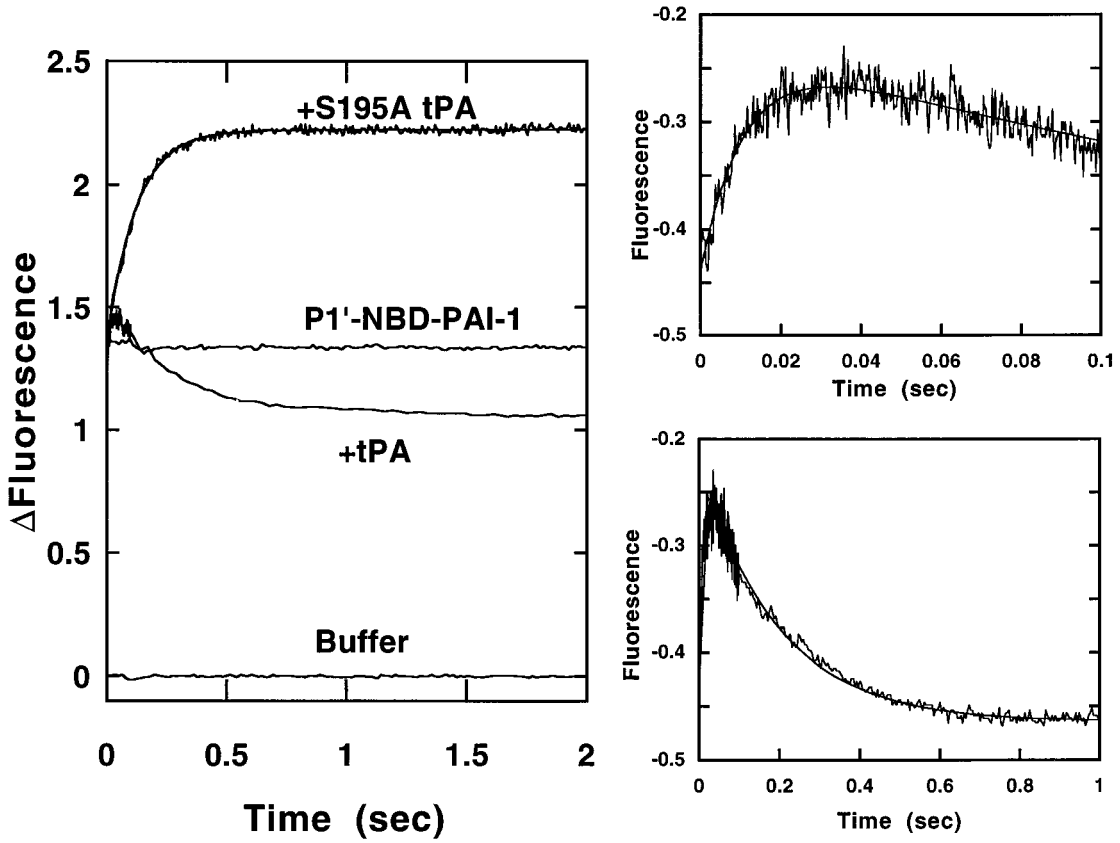

FIGURE 7: Comparison of the kinetics of S195A tPA and tPA binding to P1′-NBD-PAI-1. Shown on the left are stopped-flow traces of the rate of the fluorescence changes accompanying the binding of 0.5 μM S195A tPA or tPA to 0.1 μM P1′-NBD-PAI-1 with controls in which buffer was mixed with the fluorescent-labeled PAI-1 or with buffer. The right panels show an expanded scale representation of the reaction of 1 μM tPA with 0.1 μM P1′-NBD-PAI-1 on two time frames. Smooth solid lines are fits to a two-exponential function for the tPA reaction or to a single-exponential function for the S195A tPA reaction.

accompanying the reaction of P1′-NBD-PAI-1 with tPA together with the similarity of the fast phase change to that seen for the S195A tPA reaction demonstrated that the reaction involves an initial rapid formation of an intermediate complex resembling the noncovalent serpin−proteinase complex followed by a slower conversion of the intermediate to a covalent complex.

Analysis of the enzyme concentration dependence of the rapid exponential phase showed that k_{obs} varied linearly with enzyme concentration analogous to the linear enzyme concentration dependence of k_{obs} seen for the S195A tPA reaction (Figure 8), consistent with the fast phase representing the reversible formation of an intermediate resembling the noncovalent complex. While the slopes of the plots for tPA and S195A tPA reactions differed slightly, the intercepts showed marked differences, indicating comparable k_{on} values but ~50-fold different k_{off} values for formation of the intermediate and noncovalent complexes in tPA and S195A tPA reactions, respectively. A rigorous analysis of the biexponential reaction kinetics evident in Figures 6-8 based on the equations given in Experimental Procedures allowed all of the rate constants for the two-step reaction of tPA with P1′-NBD-PAI-1 to be determined, as shown in Scheme 1, and confirmed the validity of analyzing $k_{obs,1}$ and $k_{obs,2}$ by linear and hyperbolic equations (see Experimental Procedures). This analysis also yielded a relative fluorescence amplitude for the intermediate complex 2.5 ± 0.1-fold higher than that of the uncomplexed inhibitor, a fluorescence change similar to that found to accompany the formation of the

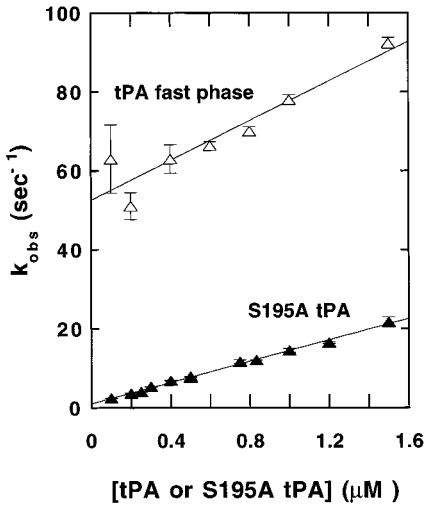

FIGURE 8: Comparison of the dependence of k_{obs} on enzyme concentration for reactions of S195A tPA and tPA with P1′-NBD-PAI-1. k_{obs} ± SE for the fast exponential phase of the tPA reaction with P1′-NBD-PAI-1 and for the single-exponential phase of the S195A tPA reaction with P1′-NBD-PAI-1 taken from Figure 5 is shown as a function of the proteinase concentration. k_{obs} was determined by fitting of data to single or double exponential functions as detailed in Experimental Procedures. Solid lines are linear regression fits of the data.

noncovalent complex of P1′-NBD-PAI-1 with S195A tPA (Figure 2).

The kinetics of labeled PAI-1 reactions with trypsin and tPA were compared with the kinetics of unlabeled wild-type

Scheme 1

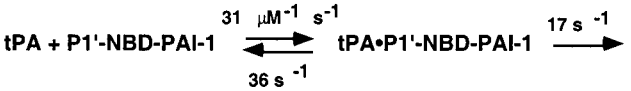

PAI-1 reactions with these enzymes by monitoring the fluorescence change accompanying the displacement of *p*-aminobenzamidine from the enzyme active-site. k_{obs} was found to increase linearly with the effective inhibitor concentration, i.e., corrected for the competitive effect of the probe, over the accessible range of such concentrations (up to ~3 μM) for both enzyme reactions (Figure 9). While this range of PAI-1 concentration was insufficient to saturate the intermediate complex in the reaction with trypsin based on the observed K_M values for the labeled PAI-1-trypsin reactions, such concentrations clearly exceeded the concentrations where intermediate complex saturation was observed to occur for the labeled PAI-1-tPA reactions. Moreover, k_{obs} values for wild-type PAI-1-tPA reactions at the highest inhibitor concentration were up to 30-fold greater than saturating values of k_{obs} seen for the labeled-PAI-1 reactions, indicating that an intermediate was not detectable when the reaction was followed from the rate of disappearance of free enzyme. Second-order association rate constants (k_{assoc}) obtained from these data were 2.8 ± 0.2 μM^{-1} s^{-1} for the trypsin reaction and 40 ± 10 μM^{-1} s^{-1} for the tPA reaction, in reasonable agreement with values obtained by monitoring loss of enzyme activity (Table 1).

DISCUSSION

Our studies have provided new insights into the nature of the noncovalent interaction between a serpin and its target proteinase and the steps involved in transforming the noncovalent complex into an inhibited covalent complex, based on a comparison of the reactions of the serpin, PAI-1, with both inactive serine 195-modified proteinases and their active counterparts. These insights were made possible by the use of previously characterized single Cys variants of PAI-1 fluorescently labeled with the environmentally sensitive fluorophore, NBD, (*4*, *7*) as probes of PAI-1 interactions with inactive and active proteinases. A key finding of our study is that the fluorescence changes induced in the labeled PAI-1 derivatives by the inactive enzymes are dramatically different from those previously shown to be induced by the active enzymes, supporting the conclusion that the covalent and noncovalent PAI-1−proteinase complexes are fundamentally different in nature. The recent structure of the α_1-proteinase inhibitor-trypsin covalent complex provides insight into the nature of such differences in that it reveals a major movement of the proteinase from its presumed site of docking with the serpin reactive center loop to the opposite end of the molecule and shows that this movement results from the burial of the cleaved serpin reactive loop and acyl-linked proteinase into β-sheet A of the serpin (*15*), in agreement with previous proposals (*4*, *7*, *25*, *39*). While there is no available structure of a noncovalent serpin−proteinase complex, such a complex is thought to have the serpin reactive center loop bound in the proteinase active site in the manner of a Michaelis complex and to resemble the lock-and-key complexes made by other protein proteinase inhibitors with their target proteinases (*14*). The fluorescence changes we observed to accompany the interaction of inactive enzymes with the labeled PAI-1 derivatives are consistent with burial of the serpin reactive center loop in the proteinase active-site in the manner of a Michaelis-like interaction. The marked differences between these changes and those shown to report reactive loop insertion into sheet A further indicates that loop insertion is not involved in forming these complexes. Anisotropy, energy transfer and intensity changes of fluorophore-labeled P1′-Cys-PAI-1 or P2′-Cys-α_1-proteinase inhibitor upon binding Ser 195-inactivated enzymes support such an interpretation (*21*, *25*). A recent NMR study of the noncovalent α_1-proteinase inhibitor−S195A trypsin complex provides further direct structural evidence that the noncovalent complex involves a lock-and-key-type interaction between a flexible serpin reactive loop and proteinase active-site resembling an enzyme−substrate complex without any significant conformational change (*26*).

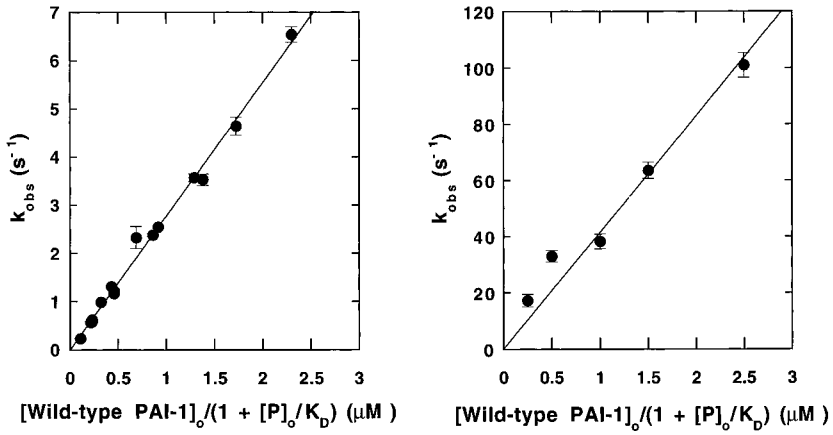

FIGURE 9: Rapid kinetics of wild-type PAI-1 reactions with trypsin and tPA monitored by *p*-aminobenzamidine displacement. Shown is the dependence of k_{obs} ± SE on the "effective" inhibitor concentration for reactions of 0.1−0.4 μM trypsin plus 10 μM *p*-aminobenzamidine (left) or of 0.1−0.4 μM tPA plus 200 μM *p*-aminobenzamidine (right) with the indicated concentrations of wild-type PAI-1. Reactions were monitored from the exponential decrease in fluorescence accompanying the displacement of *p*-aminobenzamidine from the proteinase active-site as detailed in Experimental Procedures. Effective inhibitor concentrations were calculated by dividing by the factor, $1 + [P]_o/K_D$, where $[P]_o$ represents the *p*-aminobenzamidine concentration and K_D, the dissociation constant for *p*-aminobenzamidine binding to the enzyme. Solid lines are linear regression fits of data assuming a zero intercept.

PAI-1 bound S195A tPA with >100-fold higher affinity than anhydrotrypsin, in agreement with previous work (*22*, *40*) and consistent with extended active site as well as exosite interactions being involved in recognizing the target proteinase, tPA, as compared to the relatively nonspecific proteinase, trypsin (*27*, *28*). NBD labeling of the P1′ but not the P9 residue perturbed the interaction of the PAI-1 reactive center loop with the proteinase active-site, consistent with the P1′ residue lying within the contact region with proteinase and the P9 residue being outside of this region. The limited extent of the perturbation is consistent with the broad tolerance of the S1′ site of tPA for accommodating P1′ amino acids (*41*). Noteworthy is our finding that the kinetics of binding of inactive enzymes to wild-type and labeled PAI-1s conform to a simple one-step equilibrium binding process, based on the linear dependence of k_{obs} on the enzyme or inhibitor concentration over the range of concentrations examined and on the agreement between kinetically determined and directly determined dissociation constants for the interactions. Such findings are at variance with those reported by Stone and LeBonniec (*12*) or by Mellet and Bieth (*17*) who found evidence for a two-step binding of Ser 195-inactivated proteinases to serpins based on the saturable dependence of k_{obs} on inhibitor concentration or the observation of biphasic changes in fluorescence resonance energy transfer between specifically labeled serpin but heterogeneously labeled proteinase. Our findings do not rule out a two-step binding of the inactive enzymes to the labeled PAI-1s since it is possible that a weak intermediate complex with a K_D much greater than the range of enzyme or inhibitor concentrations examined could have escaped our detection. However, they do rule out proposals made in previous studies that such a second step involves a tightening of the complex brought about through partial or full insertion of the flexible serpin reactive center loop into β-sheet A which fixes the loop in a conformation optimal for proteinase binding (*12*, *17*). Our finding that the inactive enzymes bind with somewhat higher affinity to PAI-1 derivatives in which reactive center loop insertion has been blocked thus implies that neither partial nor full loop insertion is involved in stabilizing the noncovalent PAI-1-inactive enzyme complexes and therefore that loop insertion is unlikely to be induced in these complexes. Such findings are in keeping with the previous observation that blocking loop-sheet interactions in PAI-1 does not affect Michaelis complex formation with tPA (*24*). Together, such findings suggest that proteinases bind the loop-expelled conformation of PAI-1 with the highest affinity and that the lower affinity of proteinase for native PAI-1 reflects a small fraction of native PAI-1 molecules in a partial loop-inserted state with lower proteinase affinity. Precedence for the ability of the reactive center loop of serpins to undergo such partial insertion into sheet A exists in the case of antithrombin whose reactive center loop hinge is partially inserted through the P14 residue into sheet A (*18*, *42*, *43*). This loop conformation maintains the inhibitor in a low activity state with heparin activating the serpin by inducing the expulsion of the loop from sheet A (*18*, *19*). Heparin activation is associated with a large increase in affinity of antithrombin for anhydrotrypsin (*22*), in support of the idea that the fully exposed serpin reactive loop most effectively binds proteinases.

The saturable dependence of k_{obs} on enzyme concentration for the binding of the active enzymes to the labeled PAI-1 derivatives clearly showed that an intermediate complex was formed on the pathway to the covalent complex and that the fluorescence changes reporting acylation and loop insertion were associated with conversion of the intermediate to the covalent complex and required the proteinase catalytic serine. An intermediate with fluorescence properties resembling the noncovalent complex was directly observable from the biphasic fluorescence changes accompanying the P1′-labeled PAI-1 reaction with tPA. The observation that K_M and k_{lim} values for the reactions of trypsin with P1′- or P9-labeled PAI-1 were indistinguishable implied that the events reported by the P1′- and P9-linked fluorophores occur in a common rate-determining process following noncovalent complex formation which is not affected by the fluorophore labels. This process was previously shown to be acylation based on the observation of an identical rate-determining step in the reaction of trypsin with inhibitor and substrate forms of PAI-1 and the direct demonstration by rapid quench kinetic studies of the rate-limiting accumulation and decay of the acyl-intermediate in the reaction with substrate PAI-1 (*24*). Since the P1′-fluorophore reports the separation of the P1 and P1′ amino acids following acylation of the P1 residue, an event which clearly requires cleavage of the P1−P1′ bond (*7*), it follows that the P9 fluorophore change which reports a later stage of loop insertion through the P9 residue also requires such cleavage for it to coincide with the P1′ fluorophore change. Both fluorophores thus appear to report a common loop insertion process following acylation which is limited by the rate of acylation in the case of the trypsin reaction. The finding of indistinguishable K_M values for the two labeled PAI-1 reactions with trypsin suggests that the K_M does not reflect the K_D for formation of the initial noncovalent complex, since different K_M values would have otherwise been observed for the two reactions due to the marked perturbation of the noncovalent complex K_D by the P1′ fluorophore (Table 2). The finding that k_{lim} greatly exceeds k_{off} for dissociation of the noncovalent complex (Tables 1 and 2) rather implies that $K_M = (k_{lim} + k_{off})/k_{on} \approx k_{lim}/k_{on}$ and therefore that the association rate constant for covalent complex formation, k_{lim}/K_M, is approximated by k_{on}, i.e., that association of PAI-1 and trypsin is diffusion-limited. Since the P1′ label minimally affects k_{on} for noncovalent complex formation (Table 2), K_M values for P1′ and P9-labeled PAI-1 reactions are expected to be similar. A diffusion-limited association would account for our inability to detect the noncovalent complex as a separate kinetic phase in the labeled PAI-1 reactions except at high proteinase concentrations.

Previous rapid quenching kinetic studies of the wild-type PAI-1-trypsin reaction in which SDS-stable complex formation was monitored suggested a lower k_{lim} value ($\sim$20 s^{-1}) than that measured for the labeled PAI-1-trypsin reactions in this study (80−90 s^{-1}) (*24*). Rapid kinetic studies of the antichymotrypsin-chymotrypsin reaction similarly observed a faster rate of loop insertion as reported by a P7-linked fluorophore than SDS-stable complex formation, and concluded from this that cleavage of the P1−P1′ bond occurred after loop insertion (*16*). In the context of our present findings, an alternative explanation for these observations is that an additional step after loop insertion is required for

distorting and stabilizing the proteinase as an SDS-stable complex and that this distortion step additionally limits the rate of formation of the stable complex (*6*, *15*). Direct probes of proteinase distortion will be required to verify this possibility.

Contrasting the trypsin reactions with the labeled PAI-1 species, K_M and k_{lim} values for the reactions of tPA with each labeled PAI-1 differed greatly. The origin of these differences was clarified by our ability to determine all of the rate constants for the two-step reaction of P1′-NBD-PAI-1 with tPA from the biphasic fluorescence changes observable for this reaction. The observation that the differences in K_M for the tPA reactions with the two labeled PAI-1s paralleled similar differences in K_D for formation of noncovalent complexes of the labeled PAI-1s with S195A tPA in either 0.1 or 0.5 M Hepes buffers (Tables 1 and 2) suggests that the differences in K_M reflect the perturbed binding of the P1′-labeled PAI-1 to the enzyme in the intermediate complex. This conclusion is supported by the comparable values of k_{off} and k_{lim} for intermediate complex formation in the P1′-labeled PAI-1-tPA reaction (Scheme 1), which is consistent with K_M partly reflecting the K_D for formation of the initial complex.

Surprisingly, the K_D calculated for formation of the intermediate complex between tPA and P1′-NBD-PAI-1 (36 $s^{-1}/30\ \mu M^{-1}\ s^{-1} = \sim 1\ \mu M$) indicated a ~20-fold weaker affinity for this complex than for the noncovalent complex between S195A tPA and P1′-NBD-PAI-1 (K_D 70 nM). This difference in affinity may reflect the previously demonstrated reversibility of the acylation step in the tPA-PAI-1 reaction which arises as a consequence of tPA-PAI-1 exosite interactions (*24*). These exosite interactions between positively charged residues of a tPA insertion loop and negatively charged residues in the primed end of the PAI-1 reactive center loop (*27*, *28*) make acylation reversible by impeding the release of the primed end of the cleaved PAI-1 reactive loop from the tPA active-site, as evidenced by the slow deacylation of substrate PAI-1 by tPA in previous studies (0.06 s^{-1}) (*24*). The intermediate complex we observed in the P1′-labeled PAI-1-tPA reaction with fluorescence properties resembling the noncovalent complex is thus likely to represent an equilibrium mixture of noncovalent Michaelis and covalent acyl−enzyme complexes, wherein the reactive loop is cleaved in the latter complex but maintains the conformation of the intact loop due to strong interactions of primed and unprimed sides of the loop with tPA (Scheme 2). According to such a model, the affinity of the intermediate complex with tPA is reduced from that of the noncovalent complex with S195A tPA due to acylation destabilizing the PAI-1 reactive loop interaction with tPA.

Scheme 2

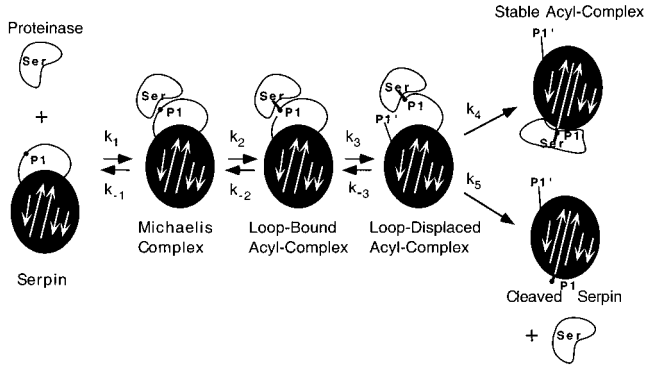

Our conclusion that the reversibly formed intermediate complex observed in the labeled PAI-1-tPA reactions represents an equilibrium mixture of Michaelis and acyl−enzyme complexes rationalizes the observation of an apparent irreversible reaction of wild-type PAI-1 with tPA with no detectable intermediate when the wild-type PAI-1-tPA reaction was monitored by the disappearance of active enzyme. The kinetics of the wild-type PAI-1-tPA covalent complex reaction paralleled that of the P9-labeled PAI-1-S195A tPA noncovalent complex reaction, implying that the rate-limiting step in the covalent reaction is the diffusion-controlled association of PAI-1 and tPA to form a tight noncovalent complex similar to that formed with S195A tPA. This complex has no opportunity to dissociate back to free enzyme and inhibitor because of an extremely low off-rate for dissociation (Table 2), in comparison to the more rapid rates of reversible acyl−enzyme formation and trapping of the acyl−enzyme complex. The disappearance of active enzyme thus appears to be irreversible with no intermediate detectable. A diffusion-limited association of PAI-1 and tPA is supported by k_{assoc} values measured for PAI-1 inhibition of active tPA by loss of enzymatic activity correlating reasonably well with k_{on} values for PAI-1 binding to S195A tPA in either 0.1 or 0.5 M Hepes buffers (Tables 1 and 2).

While present and past studies favor the view that exosite interactions function to promote an initial tight noncovalent association of PAI-1 and tPA and facilitate a reversible acylation of the loop, they are as a consequence expected to impede the release and burial of the cleaved reactive loop and tethered proteinase into sheet A (*24*). Reactive loop insertion thus becomes rate-limiting in the formation of the covalent complex as was previously shown from the large effect of blocking loop insertion on the rate-limiting step in the PAI-1 reaction with tPA but not in the reaction with trypsin where acylation is rate-determining (*24*). The k_{lim} of 3 s^{-1} observed for the reaction of wild-type PAI-1 with tPA monitored by SDS-stable complex formation in these past rapid quench kinetic studies is identical to the value obtained for the P9-labeled PAI-1-tPA reaction in the present study, consistent with k_{lim} for labeled and unlabeled PAI-1 reactions representing a common rate-limiting loop insertion step leading to the covalent complex. Our finding of a significantly greater k_{lim} value of 17 s^{-1} for the tPA reaction with P1′-NBD-PAI-1 supports the idea that k_{lim} reflects a rate-limiting burial of the reactive loop into sheet A since the P1′ fluorophore is expected to perturb the nearby exosite interactions which hinder loop insertion and thereby increase the rate of the insertion.

The present findings in conjunction with past results (*13*, *24*) thus support the mechanism shown in Scheme 2 for the PAI-1-tPA reaction. In this mechanism, a tight noncovalent Michaelis complex is initially formed in a rate-controlling diffusion-limited step. This complex subsequently undergoes a reversible acylation due to strong interactions of both primed and unprimed ends of the reactive loop with tPA. A rate-limiting reversible dissociation of the primed end of the cleaved reactive loop from the proteinase then promotes the rapid insertion of the unprimed end of the loop and tethered proteinase leading to stabilization of the acyl−enzyme complex. The conformational trapping of the acyl−enzyme

competes with a normal deacylation of the acyl-intermediate to regenerate free enzyme and release cleaved inhibitor (*13*, *24*). The minimal formation of cleaved PAI-1 in the reaction of wild-type or P1′-NBD-PAI-1 with tPA but increased formation in the P9-NBD-PAI-1 reaction implies that loop insertion is normally much faster than deacylation ($k_4 \gg k_5$), but that the P9 fluorophore slows the rate of this insertion to more closely approach the deacylation rate. However, this effect will not be reflected in k_{lim} according to the reaction model if loop insertion and deacylation are both limited by the rate of dissociation of the primed side of the PAI-1 reactive loop from the tPA exosite (k_3 step in Scheme 2). For the mechanism of Scheme 2, formation of the Michaelis complex is rate-determining for proteinase inhibition and dissociation of the primed end of the cleaved reactive loop is rate-determining for formation of the final covalent complex. Such rate-determining steps may explain the unusual pH dependence reported for some serpin−proteinase reactions which differs from the expected pH dependence for acylation (*17*, *45*).

To verify that Scheme 2 provides a satisfactory explanation for all of our data, simulations were performed using reasonable estimates of rate constants in accord with our experimental observations. Assuming that the Michaelis complex is formed in a diffusion-limited step and rapidly equilibrates with the acyl-enzyme complexes without significant dissociation (k_2, k_{-2}, k_3, $k_{-3} \gg k_{-1}$) and that dissociation of the reactive loop from the tPA exosite controls the rate of loop insertion into sheet A (k_4 and $k_5 \gg k_3$, k_{-3}), k_{lim}, k_{on}, and k_{off} for this mechanism will be given by $k_2k_3/(k_2 + k_{-2} + k_3)$, k_1, and $k_{-1}k_{-2}k_{-3}/k_2k_3$, respectively (*24*).[3] Assuming further that reversible acylation of the Michaelis complex destabilizes the complex, ($k_{-2} \gg k_2$), the simulations reproduce well the kinetic behavior we have observed for the wild-type and P9-labeled PAI-1 reactions with tPA when individual rate constants are set to $k_1 = 30\ \mu M^{-1}\ s^{-1}$, $k_{-1} = 0.03\ s^{-1}$, $k_2 = 100\ s^{-1}$, $k_{-2} = 1000\ s^{-1}$, $k_3 = 30\ s^{-1}$, $k_{-3} = 10\ s^{-1}$, $k_4 = 500\ s^{-1}$, and $k_5 = 50$ or $250\ s^{-1}$ for wild-type or P9-NBD PAI-1 reactions, respectively, i.e., they yield values for k_{on} of $30\ \mu M^{-1}\ s^{-1}$, k_{off} of $0.1\ s^{-1}$, k_{lim} of $2.6\ s^{-1}$, K_M of $\sim 0.1\ \mu M$, a K_D for the Michaelis complex of $k_{-1}/k_1 = 1$ nM and a ratio of inhibition stoichiometries for labeled vs wild-type PAI-1 reactions of 1.4. Moreover, such simulations demonstrate that disappearance of free enzyme will appear to be an irreversible bimolecular reaction with no detectable intermediate complex, whereas an intermediate will be detected when the reaction is monitored by signals which report reactive loop insertion. While this set of rate constants are not unique, the simulations support the validity of the minimal mechanism we propose and place limits on the relative values of individual rate constants. Finally, the same mechanism is followed by the PAI-1-trypsin reaction, but in this case the absence of an exosite interaction causes acylation to become effectively irreversible and rate-controlling due to the release of the constraints on the reactive loop conformational change step.

[3] Simulations verify that when the enzyme is in molar excess over the inhibitor, k_{lim} will not be sensitive to the substrate pathway when the k_3 step in Scheme 2 is rate-limiting.

ACKNOWLEDGMENT

We thank Bruce Keyt and Genentech, Inc. for generously supplying the recombinant S195A tPA and tPA. We are also grateful to Peter Gettins of the University of Illinois at Chicago for his helpful comments on the manuscript.

REFERENCES

1. Gettins, P. G. W., Patston, P. A., and Olson, S. T. (1996) *Serpins: Structure, Function and Biology*; R. G. Landes, Austin, TX.
2. Church, F. C., Cunningham, D. D., Ginsburg, D., Hoffman, M., Stone, S. R., and Tollefsen, D. M., Eds. (1997) *Chemistry and Biology of Serpins*; Plenum Press, New York.
3. Björk, I., Nordling, K., and Olson, S. T. (1993) *Biochemistry 32*, 6501−6505.
4. Shore, J. D., Day, D. E., Francis-Chmura, A. M., Verhamme, I., Kvassman, J., Lawrence, D. A., and Ginsburg, D. (1995) *J. Biol. Chem. 270*, 5395−5398.
5. Stavridi, E., O'Malley, K., Lukacs, C., Moore, W. T., Lambris, J. D., Christianson, D., Rubin, H., and Cooperman, B. S. (1996) *Biochemistry 35*, 10608−10615.
6. Kaslik, G., Kardos, J., Szabo, L., Zavodszky, P., Westler, W. M., Markely, J. L., and Graf, L. (1997) *Biochemistry 36*, 5455−5474.
7. Lawrence, D. A., Ginsburg, D., Day, D. E., Berkenpas, M. B., Verhamme, I. M., Kvassman, J., and Shore, J. D. (1995) *J. Biol. Chem. 270*, 25309−25312.
8. Wilczynska, M., Fa, M., Ohlsson, P., and Ny, T. (1995) *J. Biol. Chem. 270*, 29652−29655.
9. Egelund, R., Rodenburg, K. W., Andreasen, P. A., Rasmussen, M. S., Guldberg, R. E., and Petersen, T. E. (1998) *Biochemistry 37*, 6375−6379.
10. Olson, S. T., and Shore, J. D. (1982) *J. Biol. Chem. 257*, 14891−14895.
11. Olson, S. T. (1985) *J. Biol. Chem. 260*, 10153−10160.
12. Stone, S. R., and LeBonniec, B. F. (1997) *J. Mol. Biol. 265*, 344−362.
13. Lawrence, D. A., Olson, S. T., Kvassman, J., Ginsburg, D., and Shore, J. D. (2000) *J. Biol. Chem. 275*, 5839−5844.
14. Bode, W., and Huber, R. (1992) *Eur. J. Biochem. 204*, 433−451.
15. Huntington, J. A., Read, R. J., and Carrell, R. W. (2000) *Nature 407*, 923−926.
16. O'Malley, K., Nair, S., Rubin, H., and Cooperman, B. (1997) *J. Biol. Chem. 272*, 5354−5359.
17. Mellet, P., and Bieth, J. G. (2000) *J. Biol. Chem. 275*, 10788−10795.
18. Huntington, J. A., Olson, S. T., Fan, B., and Gettins, P. G. W. (1996) *Biochemistry 35*, 8495−8503.
19. Jin, L., Abrahams, J. P., Skinner, R., Petitou, M., Pike, R. N., and Carrell, R. W. (1997) *Proc. Natl. Acad. Sci., U.S.A. 94*, 14683−14688.
20. Mottonen, J., Strand, A., Symersky, J., Sweet, R. M., Danley, D. E., Geoghegan, K. F., Gerard, R. D., and Goldsmith, E. J. (1992) *Nature 355*, 270−273.
21. Fa, M., Karolin, J., Aleshkov, S., Strandberg, L., Johansson, L., and Ny, T. (1995) *Biochemistry 34*, 13833−13840.
22. Olson, S. T., Bock, P. E., Kvassman, J., Shore, J. D., Lawrence, D. A., Ginsburg, D., and Björk, I. (1995) *J. Biol. Chem. 270*, 30007−30017.
23. Olson, S. T., Swanson, R., Patston, P. A., and Björk, I. (1997) *J. Biol. Chem. 272*, 13338−13342.
24. Kvassman, J.-O., Verhamme, I., and Shore, J. D. (1998) *Biochemistry 37*, 15491−15502.
25. Stratikos, E., and Gettins, P. G. W. (1999) *Proc. Natl. Acad. Sci., U.S.A. 96*, 4808−4813.
26. Peterson, F. C., Gordon, N. C., and Gettins, P. G. W. (2000) *Biochemistry 39*, 11884−11892.
27. Madison, E. L., Goldsmith, E. J., Gerard, R. D., Gething, M. J. H., Sambrook, J. F., and Bassel-Duby, R. S. (1990) *Proc. Natl. Acad. Sci., U.S.A. 87*, 3530−3533.

28. Horrevoets, A. J. G., Tans, G., Smilde, A. E., van Zonneveld, A. J., and Pannekoek, H. (1993) *J. Biol. Chem. 268*, 779−782.
29. Wållen, P., Bergsdorf, N., and Rånby, M. (1982) *Biochim. Biophys. Acta 719*, 318−328.
30. Yung, B. Y., and Trowbridge, C. G. (1975) *Biochem. Biophys. Res. Commun. 65*, 927−930.
31. Ako, H., Foster, R. J., and Ryan, C. A. (1974) *Biochemistry 13*, 132−139.
32. Robinson, N. C., Tye, R. W., Neurath, H., and Walsh, K. A. (1971) *Biochemistry 10*, 2743−2747.
33. Laemmli, U. K. (1970) *Nature 227*, 680−685.
34. Latallo, Z. S., and Hall, J. A. (1986) *Thromb. Res. 43*, 507−521.
35. Lindahl, P., Raub-Segall, E., Olson, S. T., and Björk, I. (1991) *Biochem. J. 276*, 387−394.
36. Moore, J. W., and Pearson, R. G. (1981) *Kinetics and Mechanism*, pp 296−300, John Wiley & Sons, New York.
37. Bock, P. E., Day, D. E., Verhamme, I. M. A., Bernardo, M. M., Olson, S. T., and Shore, J. D. (1996) *J. Biol. Chem. 271*, 1072−1080.
38. Lawrence, D. A., Olson, S. T., Palaniappan, S., and Ginsburg, D. (1994) *J. Biol. Chem. 269*, 27657−27662.
39. Stratikos, E., and Gettins, P. G. W. (1998) *J. Biol. Chem. 273*, 15582−15589.
40. Lijnen, H. R., VanHoef, B., and Collen, D. (1991) *J. Biol. Chem. 266*, 4041−4044.
41. Sherman, P. M., Lawrence, D. A., Yang, A. Y., Vandenberg, E. T., Paielli, D., Olson, S. T., Shore, J. D., and Ginsburg, D. (1992) *J. Biol. Chem. 267*, 7588−7595.
42. Schreuder, H. A., de Boer, B., Dijkema, R., Mulders, J., Theunissen, H. J. M., Grootenhuis, P. D. J., and Hol, W. G. J. (1994) *Nat. Struct. Biol. 1*, 48−54.
43. Carrell, R. W., Stein, P. E., Fermi, G., and Wardell, M. R. (1994) *Structure 2*, 257−270.
44. Skinner, R., Chang, W.-S. W., Jin, L., Pei, X., Huntington, J. A., Abrahams, J.-P., Carrell, R. W. and Lomas, D. A. (1998) *J. Mol. Biol. 283*, 9−14.
45. Schechter, N. M., Plotnick, M., Selwood, T., Walter, M., and Rubin, H. (1997) *J. Biol. Chem. 272*, 24499−24507.

BI0107290